HHS Public Access

Author manuscript

SLAS Discov. Author manuscript; available in PMC 2019 April 01.

Published in final edited form as:

SLAS Discov. 2018 April ; 23(4): 363–374. doi:10.1177/2472555217752301.

Screen Targeting Lung and Prostate Cancer Oncogene Identifies Novel Inhibitors of RGS17 and Problematic Chemical Substructures

Christopher R. Bodle[1], **Josephine H. Schamp**[1], **Joseph B. O'Brien**[1], **Michael P. Hayes**[1], **Meng Wu**[1,2,3], **Jonathan A. Doorn**[1], and **David L. Roman**[1,4]

[1]Department of Pharmaceutical Sciences and Experimental Therapeutics, University of Iowa, Iowa City, IA 52242, United States.

[2]University of Iowa High Throughput Screening Facility (UIHTS), University of Iowa, Iowa City, IA 52242, United States.

[3]Department of Biochemistry, Carver College of Medicine, University of Iowa, Iowa City, IA 52242, United States.

[4]Cancer Signaling and Experimental Therapeutics Program, Holden Comprehensive Cancer Center, UIHC, University of Iowa, Iowa City, IA 52242, United States.

Abstract

Regulator of G protein signaling (RGS) proteins temporally regulate heterotrimeric G protein signaling cascades elicited by GPCR activation, and thus are essential for cell homeostasis. The dysregulation of RGS protein expression has been linked to several pathologies, spurring discovery efforts to identify small molecule inhibitors of these proteins. Presented here are the results of a high throughput screening (HTS) campaign targeting RGS17, an RGS protein reported to be inappropriately upregulated in several cancers. A screen of over 60,000 small molecules led to the identification of five hit compounds that inhibit the RGS17: $G\alpha_o$ protein-protein interaction. Chemical and biochemical characterization demonstrated that three of these hits inhibited the interaction through the decomposition of parent compound into reactive products under normal chemical library storage/usage conditions. Compound substructures susceptible to decomposition are reported and the decomposition process characterized, adding to the armamentarium of tools available to the screening field, allowing for the conservation of resources in follow up efforts and more efficient identification of potentially decomposed compounds. Finally, analogs of one hit compound were tested, and the results establish the first ever structure activity relationship (SAR) profile for a small molecule inhibitor of RGS17.

Keywords

RGS proteins; High throughput screening; SAR; compound decomposition; AlphaScreen

Corresponding Author: David L. Roman, College of Pharmacy, University of Iowa, 115 S. Grand Avenue, S327 PHAR, Iowa City, Iowa 52242, Tel: 319-335-6920, Fax: 319-335-8766, David-roman@uiowa.edu.

Conflicts of Interest:
The authors disclose no potential conflicts of interest.

Introduction

Activation of G protein-coupled receptor (GPCR) signaling pathways governs many cellular and physiological processes.[1–4] These processes are mediated by both heterotrimeric guanine nucleotide binding proteins (G proteins) and β-arrestins.[2, 5] Given the diverse array of signaling cascades governed by these receptors, GPCRs remain one of the most highly targeted sites of therapeutic intervention.[6]

Regulator of G protein Signaling (RGS) proteins are a class of protein that temporally regulate the heterotrimeric G protein signaling cascades elicited by GPCR activation. Upon agonist binding to the receptor, the GPCR acts as a guanine nucleotide exchange factor and promotes the exchange of guanosine diphosphate (GDP) for guanosine triphosphate (GTP) at the active site of the Gα subunit. This results in the dissociation of the G protein heterotrimer (Gαβγ) into the active Gα subunit and the Gβγ heterodimer, both of which act as effectors for unique signaling cascades.[3–4] RGS proteins bind the Gα-[GDP]-GTP transition state through a semi-conserved 120 amino acid sequence known as the RGS homology (RH) domain, and act to accelerate the GTPase activity of $G\alpha_{i/o}$ and $G\alpha_{q}$ G proteins through stabilization of the transition state and promotion of hydrolysis of the γ phosphate of GTP, thus returning Gα to its GDP bound inactive state, which promotes re-association of the Gαβγ heterotrimer and terminates the G protein signaling cascade.[7–9]

Recently, RGS proteins have been implicated in a number of pathologies, both through their function as negative regulators of G protein signaling and through G protein independent mechanisms, reviewed in [10–13]. This has led to discovery efforts utilizing high throughput screening (HTS) to discover small molecule inhibitors of these proteins, with some success.[14–18] Yet targeting these proteins with small molecules is a relatively new endeavor, with the first small molecule inhibitor of an RGS protein discovered only in 2007.[14] Therefore, there is limited knowledge with respect to characterization of small molecule binding to these proteins and mechanism of small molecule mediated inhibition of the proteins.

To date, a commonality among many RGS small molecule inhibitors is that they interact with cysteine residues located at allosteric sites with respect to the G protein binding interface.[16, 18–21] These critical cysteine residues tend to be solvent protected, and only recently have reports indicated a mechanism by which small molecule inhibitors access and bind these cysteine residues.[21] Since, via this mechanism, a putative binding pocket has only recently been suggested, and since this mechanism of inhibitor binding has not been verified for many RGS proteins, investigation of lead compound structural analogs (in the absence of molecular modeling) remains the most informative strategy to elucidate compound substructures essential for small molecule binding. Testing these lead compound analogs serves to establish a structure activity relationship (SAR) profile that will be essential in the development of RGS protein specific small molecule inhibitors. However, due to the relative infancy of targeting RGS proteins with small molecules, only one report detailing the investigation of structural analogs of RGS inhibitors has been published to date.[22]

As mentioned above, targeting RGS proteins through HTS has had some successes, with the identification of potent inhibitors of RGS4, and identification of lead compounds that demonstrate activity in several mouse models *in vivo*.[16, 23–25] Yet HTS is not without pitfalls, including identification of promiscuous small molecules that may interfere with a multitude of screening assays, as well as identification of false positives through instability of small molecules in library storage conditions.[26–29] The subject of assay interfering compounds has been extensively published, and online computational tools exist to identify putative problematic substructures in this regard.[30] However, the subject of small molecule integrity in screening libraries is much less discussed, perhaps due to these compounds being dismissed as false positives during lead molecule verification. A recent report by Olson et al. detailed the identification of a chemical structure prone to instability in screening libraries.[31] Additionally, these authors found that this chemical structure was enriched in screening libraries. Therefore, it seems in the best interest of the field to identify compound structures prone to instability to prevent the misallocation of resources toward these chemical entities.

Here we present our results of a HTS campaign targeting the RGS protein RGS17, a protein that has been reported to be upregulated in lung, prostate, breast, and hepatocellular carcinomas.[10] Mechanistic investigation of RGS17 function in these pathologies indicated that RGS17 dysregulation was altering the $G\alpha_s - G\alpha_i$ signaling balance in the cell through increased negative regulation of Gαi and promoting the increased transcription of several CRE promoted oncogenes.[10] Knockdown of RGS17 was reported to inhibit the growth of lung, prostate, and hepatocellular carcinoma cell lines in culture, and was reported to drastically reduce tumor progression in a mouse model *in vivo,* thus establishing this RGS protein as a promising therapeutic target.[10] After initial hit compound verification, five compounds were characterized for mechanism of inhibition (i.e. cysteine dependence). Three compounds were shown to lose activity when fresh stocks were prepared from commercial sources, yet recovered activity over time, indicating instability of these compounds in chemical library storage conditions. Additionally, to establish a SAR profile for targeting RGS17, analogs of one lead compound were investigated. Finally, the selectivity of the two remaining lead compounds and one compound analog with respect to other RGS proteins was assessed.

Material and Methods:

Protein Purification:

All proteins were purified as previously described.[18, 32] Concentration of active G protein was determined by GTPγ[^{35}S] binding as previously described.[18] Wild type (WT) and mutant RGS protein activity was determined previously using a Malachite Green GAP activity assay (see below).[18, 32]

AlphaScreen, Screening Campaign and Dose Response:

AlphaScreen (Perkin Elmer, Waltham, MA) was utilized largely as previously described.[18] Screening was performed in 1536 well plates (Nunc, Rochester, NY) with final concentrations of each component being 10 nM each protein (RGS and G protein) and 10

ng/μL each bead. The NCI NExT Diversity Library was screened at a final compound concentration of 35.7 μM. Due to financial constraints, only 60,502 compounds were screened from this library, representing roughly 75% coverage of the 83,536 compound collection. Dose response follow up was performed in 384 well low volume plates (Corning, Kennebunk, ME). Three point dose response assessment utilized compound final concentrations of 119 μM, 35.7 μM, and 11.9 μM. For nine point dose response assessment compound final concentrations ranged from 100 μM to 31.6 nM following a half log dilution pattern. Counter screening / assay interference control assay utilized the AlphaScreen TruHits assay (Perkin Elmer, Waltham, MA) as previously described.[18] All plates were read on an Envision plate reader (Perkin Elmer, Waltham, MA) and all data were analyzed using GraphPad Prism 7 (GraphPad, La Jolla, CA).

AlphaScreen –Screening Data Positional Bias Corrective Analysis:

During the screening campaign, it became apparent that systematic error in the screening process was resulting in positional effects in the plate (Figure S1A–S1B). These positional effects were especially noted in edge wells (row A and column 1 of Figure S1A), and potential dispenser bias was also noted (as seen in upper half of Figure S1A). This is not uncommon in screening campaigns utilizing small volume assays such as the AlphaScreen paradigm described here. Therefore, a B-score algorithm was utilized to correct for these positional effects.[33–34] The positive controls (see below - first four columns of plate, 128 wells) were included in the B-score computation since these wells serve to more accurately compute the median uninhibited value. The negative controls (see below – last four columns of plate, 128 wells) were removed from the B-score computation as these low value wells would skew the median value. To correct for positional bias in the negative controls, a B-score was computed on just the negative control section of the plate as well. Figures S1C and S1D depict the results of the B-score correction with a secondary calculation to return values on the scale of the raw output. The B-score effectively eliminated the edge effects, and as a result improved the plate Z-factor (Figure S1E and S1F, before and after B-score correction respectively, Z-factor = 0.55 and 0.85 respectively). Use of the B-score correction did not introduce positional bias in hit identification, as the hits were relatively evenly distributed across the plate (Figure S1G). Therefore, B-score corrective calculations were used throughout the analysis, and were implemented prior to calculation of each plates respective Z-factor (figure S1H).

AlphaScreen – Data Normalization and Curve Fitting Analysis:

AlphaScreen results are presented as normalized alpha signal. For each RGS, the positive control condition was RGS + $G\alpha_o$ + AMF with no inhibitor and was set to 100% (where AMF is a mixture of NaF, $MgCl_2$, $AlCl_3$, and GDP used to promote the formation of a G protein – GDP – AlF4 transition state mimic, promoting the formation of the G protein: RGS interaction, see references 7, 26, 32). The negative control condition was RGS + $G\alpha_o$ with no AMF, and was set to 0%. Compound results for each RGS were normalized with respect to the appropriate RGS. For compound concentration response experiments, curves were fit using GraphPad Prism 7 using a log(inhibitor) vs. response – Variable slope (four parameters) equation, with a constraint that the bottom of the curve must equal 0 (since data were normalized such that lack of a protein-protein interaction was 0%). Thus, the IC_{50}

value represents the point halfway between the top of the curve and the 0% threshold. 95% CI values were calculated using the default asymmetrical (likelihood) method in GraphPad Prism 7. For RGS selectivity analysis, statistical significance was determined using one way ANOVA, with Holm-Sidak post hoc multiple comparisons analysis.

Malachite Green Steady-State GTPase Assay:

Malachite Green assay was performed largely as described previously.[18] In brief, lead compounds were tested at final concentrations of 50 and 75 μM. Compounds were allowed to incubate with RGS17 for 30 minutes prior to the addition of Gαi1 (R178M, A326S) and GTP. The reaction was allowed to proceed for 75 minutes, then quenched with the addition of Developing Solution (50:12.5:1 malachite: molybdate: Tween-20). Reactions were allowed to develop for 50 minutes prior to read at 642 nm on a Biotek Synergy 2 plate reader.

Thin Layer Chromatography (TLC):

Freshly prepared compound stocks and stocks that had incubated at RT for 28 days were spotted on Uniplate Silica Gel GHLF TLC plates (Analtech, Newark, DE) and the plates were assessed for the appearance of new product bands. Compound IV was resolved using a mobile phase of 1:1 Ethyl Acetate: Hexanes. Compounds I and V were resolved using a mobile phase of 1:2 Ethyl Acetate: Hexanes. Bands were detected with UV radiation at 254 nm.

Thiol Reactivity Testing:

Lead compounds and select analog thiol reactivity was determined as previously described.[18] In short, 100 μM *N*-acetyl cysteine (NAC) was incubated with 100 μM lead compound or N-ethylmaleimide (NEM) (positive control) for 4 hours at 37°C. Following incubation, 1 mM Ellman's reagent, {5,5'[dithiobis(2-nitrobenzoic acid)]} (DTNB), was added and absorbance read at 412 nm using a Molecular Devices SpectraMax (Sunnyvale, CA) plate reader. Data were analyzed using GraphPad Prism 7 (GraphPad, La Jolla, CA). Statistical significance was determined using one way ANOVA, with Holm-Sidak post hoc multiple comparisons analysis.

Detection of compound degradation using HPLC:

Briefly, an Agilent 1200 Series Capillary HPLC system with a photodiode array detector measuring absorbance at 202 and 280 nm was used. 10 μL of sample was injected and separation was achieved using a Phenomenex Luna C18 column (1 mm × 150 mm, 100 Å) and a mobile phase consisting of (A) 0.1 % trifluoroacetic acid (v/v) in HPLC-grade water and (B) 0.1% trifluoracetic acid (v/v) in acetonitrile. A gradient was used as follows: 0–5 mins: 5% B, 5–30 mins: 5%−50% B, 30–35 mins: 50%−80% B, 35–40 mins: 80% B, 40–45 mins: 80% - 5% B, 45–60 mins: 5% B at a flow rate of 50 μl/min.

Small Molecules:

Compounds I and IV were obtained from ChemBridge Corporation (San Diego, CA). Compound V was obtained from Chemical Diversity (San Diego, CA). Compound II-7 was

obtained from Key-Organics (Camelford, Cornwall PL32 9RA, UK). Compounds II, II-1 – II-6, and III were obtained from Vitas-M Laboratory (Champaign, IL).

Results and Discussion

Identification of lead compounds:

Roughly 60,000 compounds were screened from the NCI NExT Diversity Collection to identify inhibitors of the RGS17: $G\alpha_o$ protein-protein interaction. Each plate screened contained internal positive and negative controls to ensure assay robustness and data quality. Assay robustness was assessed via Z-factor calculation.[35] Average Z-factor throughout screening campaign was calculated to be 0.68 (Figure S1H), indicating the assay was robust throughout the campaign.

131 compounds were identified as initial hits that inhibited the RGS17: $G\alpha_o$ interaction by 50% or greater at the screening concentration (Table SI). The hit compound structures were first analyzed computationally, assessing the compound substructures for the presence of putative assay interfering moieties (PAINS).[26] This was accomplished through implementation of the open source chemoinfomatics software RDKit and python script. It should be noted that an examination of the accuracy of RDKit for identification of PAINS in 2011 by Saubern et al. determined that RDKit consistently under matched or failed to match substructures compared to use of Sybyl Line Notation (SLN) (i.e. the method used in the original computational design).[36] However, in 2015 G. Landrum (RDKit) detailed that a reason for RDKits under performance was likely a function of use of SMARTS notation, and specifically the way that explicit hydrogens are handled using SMARTS.[37] Landrum showed that by merging explicit hydrogens to the query filter, a filter that previously went un-identified would now be correctly identified.[37] Finally, Landrum noted that 391 of the 480 PAINS SMARTS notations contain an explicit hydrogen, and that many of these would not generate expected matches without explicit hydrogens merged. Therefore, we included merging of explicit hydrogens to the query filter as part of our filtration script, and tested this script against the same 10,000 compound reference set utilized and made available by Saubern et al. in their original assessment of RDKit (results Table SII).[36, 38] Merging of explicit hydrogens to the query filter significantly improved the performance of substructure match identification for RDKit. The number of filters producing over matching or under matching remained consistent (although the filters producing the over/under match results changed), but more importantly the number of filters producing equivalent matches increased from only 21 (31 – no 3 pass filtration) to 115.[36] These results indicate that merging explicit hydrogens results in a filter identification rate of greater than 90% (compared to just 29% in the absence of merged hydrogens), and an equivalent filter identification rate of 75% (compared to just 14% in the absence of merged hydrogens). Thus, since the purpose of PAINS identification was for informatics purposes and not used as an exclusionary measure (see below), we utilized RDKit for PAINS identification.

Of the 131 initial hit compounds, only 21 were flagged as containing putative assay interfering structures. This pre-filtration was not used as an exclusionary method to triage compounds from further characterization, but rather as an informatics tool to identify those compounds that may cause assay interference and thus may indicate reactive substructures.

Indeed, a recent investigation of publically available screening data demonstrated that many compounds containing PAINS flagged substructures did not exhibit a greater degree of assay promiscuity.[39] However, the original report outlying these substructure filters postulates that many PAINS compounds may not solely interfere with assay mechanics, but rather that these compounds may be reactive, protein modifying compounds.[26] For this reason, it was deemed prudent to identify the hit compounds that contain these flagged substructures while not excluding said compounds from initial characterization.

Therefore, the 131 hit compounds were then assessed via 3 point dose response analysis to confirm hit compound activity and assess hits for AlphaScreen assay interference. Compounds were tested against both the protein-protein interaction and against a biotinylated GST control assay.

This control assay (TruHits, PerkinElmer) utilizes a biotinylated GST construct that can conjugate to both the streptavidin donor bead and the anti-GST acceptor bead. This results in a robust interaction response despite a lower concentration of protein utilized (10 nM final for RGS and G protein, 300 pM final for biotinylated GST).[18] Use of this assay identifies compounds that interfere with the chemistry or read out of the AlphaScreen assay (i.e., color quenchers, singlet oxygen quenchers, biotin mimetics, etc.) and thus eliminates false positives of these mechanisms. Additionally, the discrepancy in protein concentration is not as issue here as the compound concentration range remains constant, and indeed the control assay exhibits increased sensitivity since the protein concentration utilized is lower. Therefore, a compound that does not inhibit the control assay, but does inhibit the RGS: G protein interaction can be deemed a true positive hit.

For compounds to be selected for additional investigation, the hits had to demonstrate both 50% inhibition of the protein-protein interaction by a compound concentration of 100 μM and selectivity over the control assay. There were 36 compounds that met both criteria and were then investigated in a more complete concentration response manner. These were tested in three trials, with compounds triaged after each trial based on potency. Of these 36, 16 compounds were tested in n=3 (Figure S2, Table SIII). The 5 most potent compounds were selected for additional investigation (Figure 1). These 5 lead compounds were first tested in a secondary inhibition assay utilizing a previously described Malachite Green steady-state GTPase paradigm. None of the compounds inhibited the GTPase activity of RGS17 in this assay (data not shown), however it should be noted that the Malachite Green assay utilizes 100–1000 fold more RGS protein and G protein than the AlphaScreen paradigm while maintaining comparable compound concentrations. Therefore, the apparent lack of inhibition in the GTPase assay is likely due to the large shift in protein concentration utilized and may not reflect lack of compound activity.

With lead compounds in hand, the structures were reassessed for assay interfering moieties. Compounds I and III were flagged as containing putative PAINS structures, while compounds II, IV, and V did not. Therefore, compounds II, IV, and V represent the first small molecules identified by our lab that inhibit RGS17 and do not contain PAINS flagged substructures.

Lead compounds inhibit through cysteine dependent mechanism:

Previous screening campaigns targeting both RGS4 and RGS17 have predominantly identified compounds that inhibit through interaction with cysteine residues, and use of mutant RGS proteins lacking cysteine residues results in a dramatic decrease in potency of the compounds. Therefore, the newly identified lead compounds were tested for their dependency on cysteine to inhibit RGS17 (Figure 2). All five lead compounds lost inhibitory activity when tested against a cysteine null mutant (RGS17 C117A). This indicates that these compounds impart inhibition of RGS17 through interaction with this cysteine residue, either through dependence on cysteine for proper binding coordination or via direct modification of the thiol. These results also suggest that the lead compounds bind RGS17 and not the G protein. The C117A mutation does not alter RGS17s ability to bind to the G protein or alter RGS17s GAP activity.[18] Therefore, if the lead compounds bound to the G protein to impart inhibition one would expect that the compounds would disrupt the protein-protein interaction even when utilizing RGS17 C117A. This is not the case and so suggest that the compounds are binding RGS17. Additionally, these data indicate that these lead molecules are inhibiting allosterically, as Cys 117 is not at the G protein interaction interface (Figure 2). This allosteric mechanism of inhibition is also a commonality among RGS protein inhibitors to date, and indeed no published RGS inhibitors bind at the G protein interaction interface.[16, 19–21] Interestingly, Cys 117 represents the cysteine residue in RGS17 that is highly conserved among many RGS proteins. For the RGS protein RGS4, this residue corresponds to Cys 95, which was the cysteine residue at the focal point of a recent conformational dynamics study that demonstrated a mechanism by which inhibitors might access this solvent protected cysteine in RGS4 and identified a putative binding pocket at this site for RGS4.[21] Thus, the result that these lead compounds inhibit through interaction with Cys 117 in RGS17 may serve as indirect evidence that RGS17 exhibits similar conformational dynamics which allow access to this solvent protected cysteine residue. However, the investigation required to verify such a hypothesis (i.e. extensive molecular dynamics modeling and protein NMR) were outside the scope of this work.

Compounds I, IV, and V inhibit through reactive decomposition products:

In preparation for further characterization of compound mechanism of action, lead compounds were ordered from commercial sources and tested for activity. Compounds II and demonstrated comparable activity to the NCI provided stocks when prepared fresh from powder (data not shown). However, compounds I, IV, and V demonstrated almost no inhibitory activity with the freshly prepared DMSO stocks. Examination of the structure of compound IV reveals a methyl furan – quinoline substructure. This core structure has been reported to undergo time-dependent decomposition when incubated in 100% DMSO at RT, which resulted in an increase in compound potency against the target being studied.[31] Olson et al. utilized LC-MS to characterize these decomposition products, identifying at least five potential decomposition products stemming from cycloaddition at the furan forming an endoperoxide that can undergo additional transformations. Two of these transformations result in the formation of α,β unsaturations through hydrolytic opening of the endoperoxide resulting in the formation of fumarate moieties.[31]

Since the core of compound IV (Figure 3B) is highly similar to the core of the compounds tested by Olson et al., and since the three compounds that lost activity when made fresh from powder (Compounds I, IV, and V) all contain either methyl furan or furan moieties (Figure 3A–3C), it was hypothesized that these compounds may be subject to the same degradation process as outlined by Olson et al. To test this, the freshly made stocks of compounds I, IV, and V were incubated at RT and the activity was tested weekly (Figure 3, D–F). Compounds IV and V recovered inhibitory activity after just seven days of incubation, while compound I recovered activity to initial follow up levels after 14 days of incubation (Table SIV). This incubation process did not appreciably increase potency for compound I compared to initial follow up efforts with NCI provided stocks, but both compound IV and compound V demonstrated increased potency compared to that determined in initial follow up efforts. This increase in potency was indeed due to increased inhibition of the RGS17: $G\alpha_o$ interaction and not due to an increase in inhibition of the assay itself, as demonstrated by assessment of assay inhibition at the 14 day time point. None of the compounds inhibited the biotinylated GST control assay at 14 days of decomposition.

As mentioned above, Olson and colleagues identified at least five distinct decomposition products, some of which form reactive products containing α,β unsaturations and α,β unsaturated aldehydes.[31] Given that compound decomposition results in the formation of reactive products, and given that initial follow-up efforts demonstrated that all lead compounds inhibited through interaction with cysteine, it was hypothesized that the increase in potency over time observed for compounds I, IV, and V was due to an increase in reactivity with cysteine. To test this hypothesis, Ellman's reagent (5,5' –dithiobis(2-nitrobenzoic acid), DTNB) was used to assess the thiol reactivity of decomposition products at each time point. When incubated for 4h using a 1:1 molar ratio of compound: *N*-acetyl cysteine (NAC), compounds I, IV, and V demonstrated an increase in thiol reactivity corresponding to length of time allowed for compound decomposition (Figure 3G–I). This indicates that the decomposition of these compounds in DMSO form reactive products which likely contribute to the increase in inhibition observed.

To assess whether these compounds were forming a single decomposition product, or if they were indeed forming multiple products as was seen by Olson et al.,[31] TLC and HPLC methodologies were employed. Assessment of the t = 0 and t = 28 days products for each of the three compounds by TLC demonstrated drastic changes in product migration with the mobile phase (Figure S3). Compounds I and V demonstrated a reduction in intensity of the primary product from t = 0 to t = 28 days, and also demonstrated a diffuse product band on TLC for the t = 28 days sample indicating the presence of multiple decomposition products. Compound IV also demonstrated a diffuse product band and the formation of a product band not present in the t = 0 sample. Compound decomposition was also assessed using HPLC (Figure S4). Compound I t = 0 product elutes as a single peak with a retention time of 36.93 min (Figure S4A). Assessment of t = 7 days sample demonstrates the formation of multiple products with elution times ranging from 15.5 min to 36.93 min (Figure S4B). Additionally, the elution peak at 36.93 min demonstrates peak splitting that is not present in the t = 0 sample. Assessment of t = 14 days sample demonstrates an increase in intensity of the peaks that emerged at 7 days of decomposition (Figure S4C), a trend that continues for the t = 28 days sample (Figure S4D). Compound IV t = 0 product already demonstrates a degree of

heterogeneity between the major elution peak (34.63 min) and multiple low intensity peaks (Figure S4E). At seven days of decomposition, the major elution peak shifts to 38.49 minutes, indicating a unique compound from that at t = 0 (Figure S4F). Assessment of t = 14 days for compound IV demonstrates an increase in intensity for multiple products with elution times ranging from 30.69 to 38.46 min (Figure S4G). The relative intensities of these peaks remain consistent from 14 days to 28 days of decomposition (Figure S4H). Finally, compound V t = 0 product elutes as primarily a single peak with a retention time of 40.95 min (Figure S4I). Assessment of t = 7 days decomposition sample demonstrates the emergence of multiple products (Figure S4J). Of note is the peak at 43.59 min, which is the second most intense peak at this time point. Assessment of t = 14 days decomposition sample demonstrates a near total reduction of the original elution peak and a corresponding increase in intensity for the peak at 43.57 min (Figure S4K). Finally, assessment of the t = 28 days decomposition sample for compound V (Figure S4L) demonstrates that the product corresponding to the peak at 43.6 min is the primary compound product, with only a few other low intensity product peaks detected.

The TLC and HPLC analyses indicate that compounds I, IV, and V are decomposing in DMSO into multiple products. The results for compound IV are in agreement with the results describing decomposition of furan quinolines by Olson et al.,[31] however this is the first report of such decomposition for scaffolds such as compounds I and V. Assessment of thiol reactivity suggests that the decomposition results in the formation of reactive molecules, and correlates to the increase in potency observed for the disruption of the RGS17: $G\alpha_o$ interaction. It is likely that the products responsible for inhibition are either the α,β unsaturation containing fumarate compounds, or an aldehyde containing product. Given that multiple decomposition products were formed, and given that these compounds likely inhibit through mechanisms that make the compounds susceptible to off target effects, the exact identities of the decomposition products and identification of the active product(s) were not determined.

Stability of small molecule libraries is an often discussed yet rarely published debate for labs that utilize HTS.[27–28] An investigation by Zitha-Bovens et al. with respect to stability of screening compounds demonstrated that a significant number of compounds were unstable in either DMSO or DMSO/H2O, even when stored at −20 °C.[27] This work represented the establishment of an online predictor tool for compound stability, a tool that was expanded upon by Liu et al. to establish the online compound stability predictor ChemStable.[29] However, assessment of the structures of compounds I, IV, and V using this online tool indicated that each of these compounds are predicted to be stable and not likely to decompose.[29] Yet we clearly observe decomposition with these compounds when stored at RT for just one week, and our results in comparing initial follow up assessment to freshly prepared stocks indicate that these compounds are susceptible to decomposition under normal library storage conditions. This work, as well as that detailed by Olson et al.,[31] indicate that rigorous verification is required for lead molecules that contain methyl furan and furan functionalities, as compounds containing these subgroups appear susceptible to decomposition in DMSO and form reactive products.

Compound II exhibits SAR, selectively inhibit RGS17:

As a drug target, RGS proteins have only recently been the focus of discovery efforts. Indeed, the first small molecule inhibitor of RGS proteins was only discovered in 2007 in a screen targeting RGS4.[14] Consequently, reports detailing structural characterization of small molecule binding to RGS proteins remain limited.[19, 21] Structure activity relationship (SAR) studies would help characterize the binding pocket(s) for these molecules, providing critical information for the design of future RGS protein inhibitors. To date, only one report has detailed SAR with respect to an RGS inhibitor, the RGS4 inhibitor CCG-50014.[22]

In an effort to establish a small molecule binding profile for RGS17, analogs of compound II were tested for their ability to inhibit the RGS17: $G\alpha_o$ interaction (Figure 4). These compounds were selected to test distinct structural features of the parent compound and based on commercial availability. IC_{50} values for the compounds tested are listed in Table SV. Only three of the seven analogs inhibited the protein-protein interaction, with compounds II-1 and II-2 demonstrating less potent inhibition compared to the parent compound, and compound II-3 demonstrating more potent inhibition (Figure 5A–B).

Given that the parent compound II lost activity when tested against the cysteine null RGS17 mutant (Figure 2) which indicates that the compound is inhibiting through interaction with cysteine, it was assessed whether compound II-3 was a more potent RGS17: Ga interaction inhibitor due to an increased thiol reactivity (Figure 5C). Compounds II, II-3, and III were assessed for thiol reactivity in a similar manner as above. Although compounds II and II-3 trended to have a degree of thiol reactivity, none of these three compounds deviated significantly from *N*-acetyl cysteine control. Importantly, substitution of the chlorine in compound II for a bromine in compound II-3 did not result in an increase in thiol reactivity. This indicates that the increase in potency observed for compound II-3 is not due to an increase in compound reactivity, but rather may be due to preferential conformation.

Having established that compounds II, II-3, and III inhibit the interaction of RGS17 and $G\alpha_o$, it was next assessed whether the compounds were selective inhibitors of RGS17 or if they had similar inhibitory activity targeting other RGS proteins (Figure 6). The lead compounds were again tested against RGS17 along with RGS7, RGS10, and RGS18 using AlphaScreen at a final compound concentration of 31.6 μM (a concentration greater than the IC_{50} of each compound for RGS17 (Figure 6)). In each case, the compounds inhibited RGS17 to a greater degree than the other RGS proteins tested (significance determined via one-way Anova, $F(3, 8) = 53.68$, $p < 0.001$ for compound II, $F(3, 8) = 81.29$, $p < 0.001$ for compound II-3, and $F(3, 8) = 88.27$, $p < 0.001$ for compound III). Thus, these three lead compounds demonstrate selectivity in inhibiting RGS17 over these other RGS proteins tested.

The identification of compound II-3 represents the first report of compound SAR in the targeting of RGS17. Our investigation was limited due to the commercial availability of similar compounds. Therefore, a more in depth synthetic investigation involving analogs of compound II is required to further probe important binding contacts for this compound. The presence of electron withdrawing substitutions appears to be essential for the compound to impart inhibition, as substitution with electron donating groups as with compound II-1 and

II-2 result in reduced inhibitory activity. Since a common mechanism of RGS inhibitors is the covalent modification of or dependence on cysteine residues,[15–18, 21] it is notable that compound II-3 demonstrated increased potency while exhibiting no corresponding increase in thiol reactivity, leading to the deduction that increased potency is not merely due to compound II-3 being more reactive, but rather through improved recognition or binding to a site on RGS17. While the parent compound II did lose activity against the cysteine null mutant, the result with compound II-3 indicates that there exists a degree of structural specificity that imparts compound inhibition.

Recent work focused on another RGS protein, RGS4, detailed a mechanism by which RGS proteins may be inhibited at allosteric cysteine residues.[21] Specifically, the conformational dynamics of RGS4 allowed the a5-a6 helix pair of this protein to swing out and cause the protein to adopt a high energy open-like conformation, which allowed the RGS4 inhibitor CCG-50014 to bind the solvent protected critical cysteine residue. Inhibitor binding then disrupts the RGS4: Ga protein-protein interaction by preventing RGS4 from reverting to the “closed” conformation and interfering with the formation of critical binding contacts at the G protein interaction interface.[21] If RGS17 is inhibited via a similar manner, then the presence of the larger halogen in compound II-3 may result in increased potency because it traps RGS17 in a more “open” conformation than the chlorine containing compound II. More work needs to be done, potentially through molecular dynamic simulations and protein NMR, to determine the mechanism by which inclusion of the bromine in compound II-3 imparts increased potency.

In conclusion, 5 hit compounds were identified from a screen of over 60,000 compounds that inhibited the RGS17: $G\alpha_o$ protein-protein interaction with low single to double digit micro-molar IC50s. Three of these compounds were shown to lose activity when freshly prepared, and the interaction was actually inhibited by reactive decomposition products of the parent compounds. This work, along with the work by Olson et al.,[31] indicate that furan functionalities may be sensitive to decomposition in library storage and usage conditions, and as such rigorous follow up should be applied to lead compounds containing furan substructures. We also report the identification of compound II-3 through a small-scale SAR cohort, resulting in the first ever compound SAR for small molecules targeting RGS17. This compound, along with compound II and III were shown to be selective inhibitors of RGS17. With respect to the SAR study, the scope of analogs tested was limited due to commercial availability, however this work indicates conformational compound selectivity is observable in targeting RGS proteins with small molecules. A more comprehensive investigation of SAR with respect to compound II through synthetic means, as well as structural characterization of inhibitor binding are essential in the establishment of critical binding contacts at the allosteric binding site that will allow for the design of RGS17 specific small molecule inhibitors.

Supplementary Material

Refer to Web version on PubMed Central for supplementary material.

Acknowledgements

Financial support

This work was supported by NIH 5RO1CA160470 (DLR), UIowa IRG-77-004-31 (DLR), UIowa Oberley Award Seed Grant (DLR), the American Foundation for Pharmaceutical Education Predoctoral Fellowship (CRB, MPH), the NIH T32 grant 2T32GM008365-26A1(JBO), the University of Iowa Center for Biocatalysis and Bioprocessing (JBO), and the University of Iowa College of Pharmacy.

References

1. Marinissen MJ; Gutkind JS, G-protein-coupled receptors and signaling networks: emerging paradigms. Trends Pharmacol. Sci 2001, 22, 368–376. [PubMed: 11431032]
2. Pierce KL; Lefkowitz RJ, Classical and new roles of beta-arrestins in the regulation of G-protein-coupled receptors. Nat. Rev. Neurosci 2001, 2, 727–733. [PubMed: 11584310]
3. Gilman AG, G proteins: transducers of receptor-generated signals. Annu. Rev. Biochem 1987, 56, 615–649. [PubMed: 3113327]
4. Freissmuth M; Casey PJ; Gilman AG, G proteins control diverse pathways of transmembrane signaling. FASEB J 1989, 3, 2125–2131. [PubMed: 2546847]
5. Wisler JW; Xiao K; Thomsen AR, et al., Recent developments in biased agonism. Curr. Opin. Cell Biol 2014, 27, 18–24. [PubMed: 24680426]
6. Pierce KL; Premont RT; Lefkowitz RJ, Seven-transmembrane receptors. Nat. Rev. Mol. Cell Biol 2002, 3, 639–650. [PubMed: 12209124]
7. Tesmer JJ; Berman DM; Gilman AG, et al., Structure of RGS4 bound to AlF4--activated G(i alpha1): stabilization of the transition state for GTP hydrolysis. Cell 1997, 89, 251–261. [PubMed: 9108480]
8. Ross EM; Wilkie TM, GTPase-activating proteins for heterotrimeric G proteins: regulators of G protein signaling (RGS) and RGS-like proteins. Annu. Rev. Biochem 2000, 69, 795–827. [PubMed: 10966476]
9. Siderovski DP; Willard FS, The GAPs, GEFs, and GDIs of heterotrimeric G-protein alpha subunits. Int. J. Biol. Sci 2005, 1, 51–66. [PubMed: 15951850]
10. Hayes MP; Roman DL, Regulator of G Protein Signaling 17 as a Negative Modulator of GPCR Signaling in Multiple Human Cancers. AAPS J 2016, 18, 550–559. [PubMed: 26928451]
11. Hurst JH; Hooks SB, Regulator of G-protein signaling (RGS) proteins in cancer biology. Biochem. Pharmacol 2009, 78, 1289–1297. [PubMed: 19559677]
12. Sjogren B, Regulator of G protein signaling proteins as drug targets: current state and future possibilities. Adv. Pharmacol 2011, 62, 315–347. [PubMed: 21907914]
13. Sjogren B; Neubig RR, Thinking outside of the “RGS box”: new approaches to therapeutic targeting of regulators of G protein signaling. Mol. Pharmacol 2010, 78, 550–557. [PubMed: 20664002]
14. Roman DL; Talbot JN; Roof RA, et al., Identification of small-molecule inhibitors of RGS4 using a high-throughput flow cytometry protein interaction assay. Mol. Pharmacol 2007, 71, 169–175. [PubMed: 17012620]
15. Roman DL; Ota S; Neubig RR, Polyplexed flow cytometry protein interaction assay: a novel high-throughput screening paradigm for RGS protein inhibitors. J. Biomol. Screen 2009, 14, 610–619. [PubMed: 19531661]
16. Blazer LL; Zhang H; Casey EM, et al., A nanomolar-potency small molecule inhibitor of regulator of G-protein signaling proteins. Biochemistry 2011, 50, 3181–3192. [PubMed: 21329361]
17. Storaska AJ; Mei JP; Wu M, et al., Reversible inhibitors of regulators of G-protein signaling identified in a high-throughput cell-based calcium signaling assay. Cell. Signal 2013, 25, 2848–2855. [PubMed: 24041654]
18. Bodle CR; Mackie DI; Hayes MP, et al., Natural Products Discovered in a High-Throughput Screen Identified as Inhibitors of RGS17 and as Cytostatic and Cytotoxic Agents for Lung and Prostate Cancer Cell Lines. J. Nat. Prod 2017.

19. Roman DL; Blazer LL; Monroy CA, et al., Allosteric inhibition of the regulator of G protein signaling-Galpha protein-protein interaction by CCG-4986. Mol. Pharmacol 2010, 78, 360–365. [PubMed: 20530129]
20. Blazer LL; Roman DL; Chung A, et al., Reversible, allosteric small-molecule inhibitors of regulator of G protein signaling proteins. Mol. Pharmacol 2010, 78, 524–533. [PubMed: 20571077]
21. Vashisth H; Storaska AJ; Neubig RR, et al., Conformational dynamics of a regulator of G-protein signaling protein reveals a mechanism of allosteric inhibition by a small molecule. ACS Chem. Biol 2013, 8, 2778–2784. [PubMed: 24093330]
22. Turner EM; Blazer LL; Neubig RR, et al., Small Molecule Inhibitors of Regulator of G Protein Signalling (RGS) Proteins. ACS Med. Chem. Lett 2012, 3, 146–150. [PubMed: 22368763]
23. Blazer LL; Storaska AJ; Jutkiewicz EM, et al., Selectivity and anti-Parkinson's potential of thiadiazolidinone RGS4 inhibitors. ACS Chem. Neurosci 2015, 6, 911–919. [PubMed: 25844489]
24. Yoon SY; Woo J; Park JO, et al., Intrathecal RGS4 inhibitor, CCG50014, reduces nociceptive responses and enhances opioid-mediated analgesic effects in the mouse formalin test. Anesth. Analg 2015, 120, 671–677. [PubMed: 25695583]
25. Bosier B; Doyen PJ; Brolet A, et al., Inhibition of the regulator of G protein signalling RGS4 in the spinal cord decreases neuropathic hyperalgesia and restores cannabinoid CB1 receptor signalling. Br. J. Pharmacol 2015, 172, 5333–5346. [PubMed: 26478461]
26. Baell JB; Holloway GA, New substructure filters for removal of pan assay interference compounds (PAINS) from screening libraries and for their exclusion in bioassays. J. Med. Chem 2010, 53, 2719–2740. [PubMed: 20131845]
27. Zitha-Bovens E; Maas P; Wife D, et al., COMDECOM: predicting the lifetime of screening compounds in DMSO solution. J. Biomol. Screen 2009, 14, 557–565. [PubMed: 19483143]
28. Engeloch C; Schopfer U; Muckenschnabel I, et al., Stability of screening compounds in wet DMSO. J. Biomol. Screen 2008, 13, 999–1006. [PubMed: 19029012]
29. Liu Z; Zheng M; Yan X, et al., ChemStable: a web server for rule-embedded naive Bayesian learning approach to predict compound stability. J. Comput. Aided Mol. Des 2014, 28, 941–950. [PubMed: 25031075]
30. Lagorce D; Sperandio O; Baell JB, et al., FAF-Drugs3: a web server for compound property calculation and chemical library design. Nucleic Acids Res 2015, 43, W200–207. [PubMed: 25883137]
31. Olson ME; Abate-Pella D; Perkins AL, et al., Oxidative Reactivities of 2-Furylquinolines: Ubiquitous Scaffolds in Common High-Throughput Screening Libraries. J. Med. Chem 2015, 58, 7419–7430. [PubMed: 26358009]
32. Hayes MP; Bodle CR; Roman DL, Evaluation of the Selectivity and Cysteine-Dependence of Inhibitors Across the Regulator of G Protein Signaling Family. Mol. Pharmacol 2017.
33. Dragiev P; Nadon R; Makarenkov V, Two effective methods for correcting experimental high-throughput screening data. Bioinformatics 2012, 28, 1775–1782. [PubMed: 22563067]
34. Brideau C; Gunter B; Pikounis B, et al., Improved statistical methods for hit selection in high-throughput screening. J. Biomol. Screen 2003, 8, 634–647. [PubMed: 14711389]
35. Zhang JH; Chung TD; Oldenburg KR, A Simple Statistical Parameter for Use in Evaluation and Validation of High Throughput Screening Assays. J. Biomol. Screen 1999, 4, 67–73 [PubMed: 10838414]
36. Saubern S; Guha R; Baell JB, KNIME Workflow to Assess PAINS Filters in SMARTS Format. Comparison of RDKit and Indigo Cheminformatics Libraries. Mol. Inform 2011, 30, 847–850 [PubMed: 27468104]
37. Landrum G Curating the PAINS filters http://rdkit.blogspot.com/2015/08/curating-pains-filters.html.
38. Guha R PAINS Substructure Filters as SMARTS http://blog.rguha.net/?p=%20850.
39. Capuzzi SJ; Muratov EN; Tropsha A, Phantom PAINS: Problems with the Utility of Alerts for Pan-Assay INterference CompoundS. J. Chem. Inf. Model 2017.

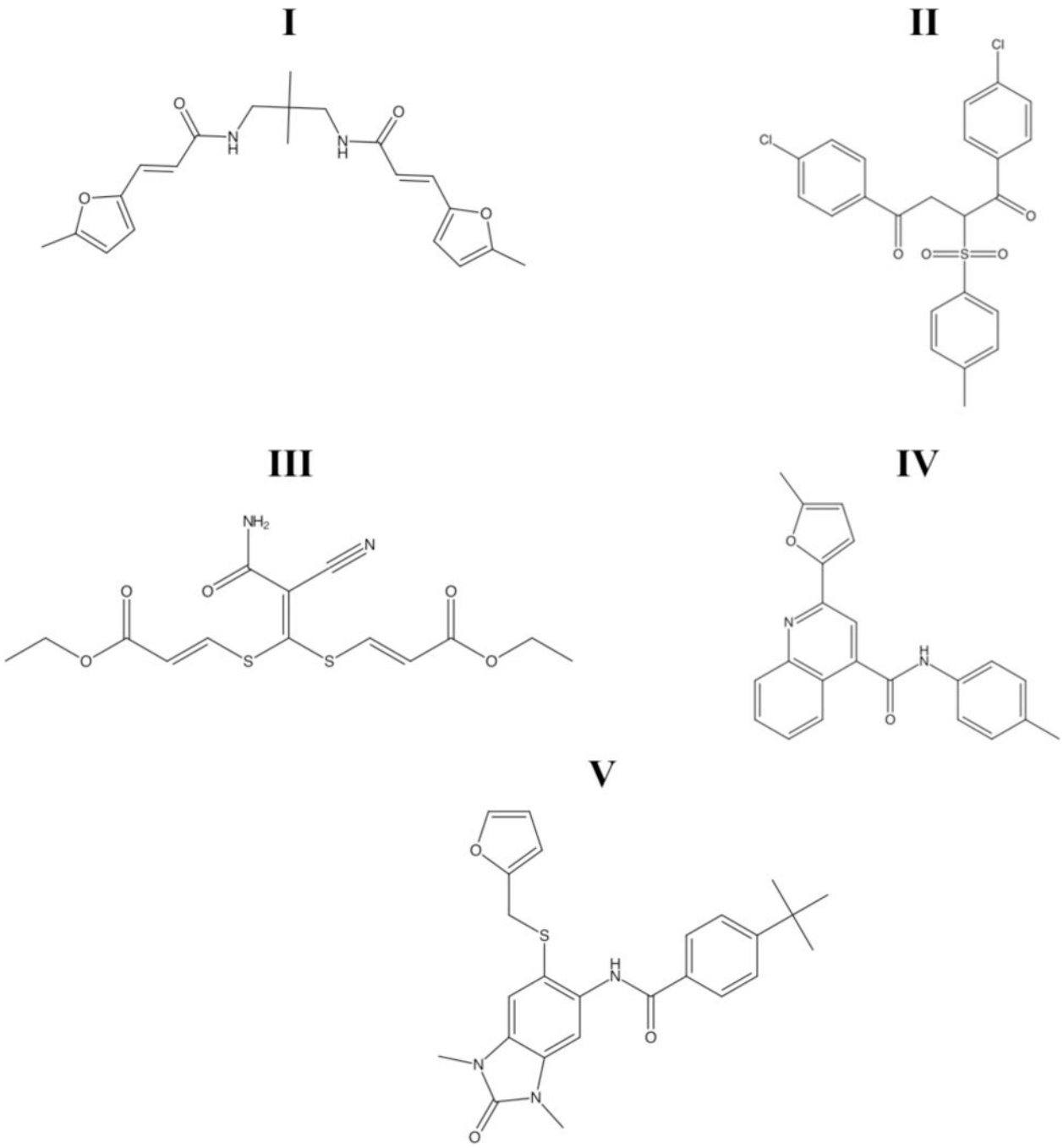

Figure 1 –.

Structures of the five lead compounds selected for characterization based on initial follow up. Compounds will be referred to in text by their respective numeric identifiers, I–V.

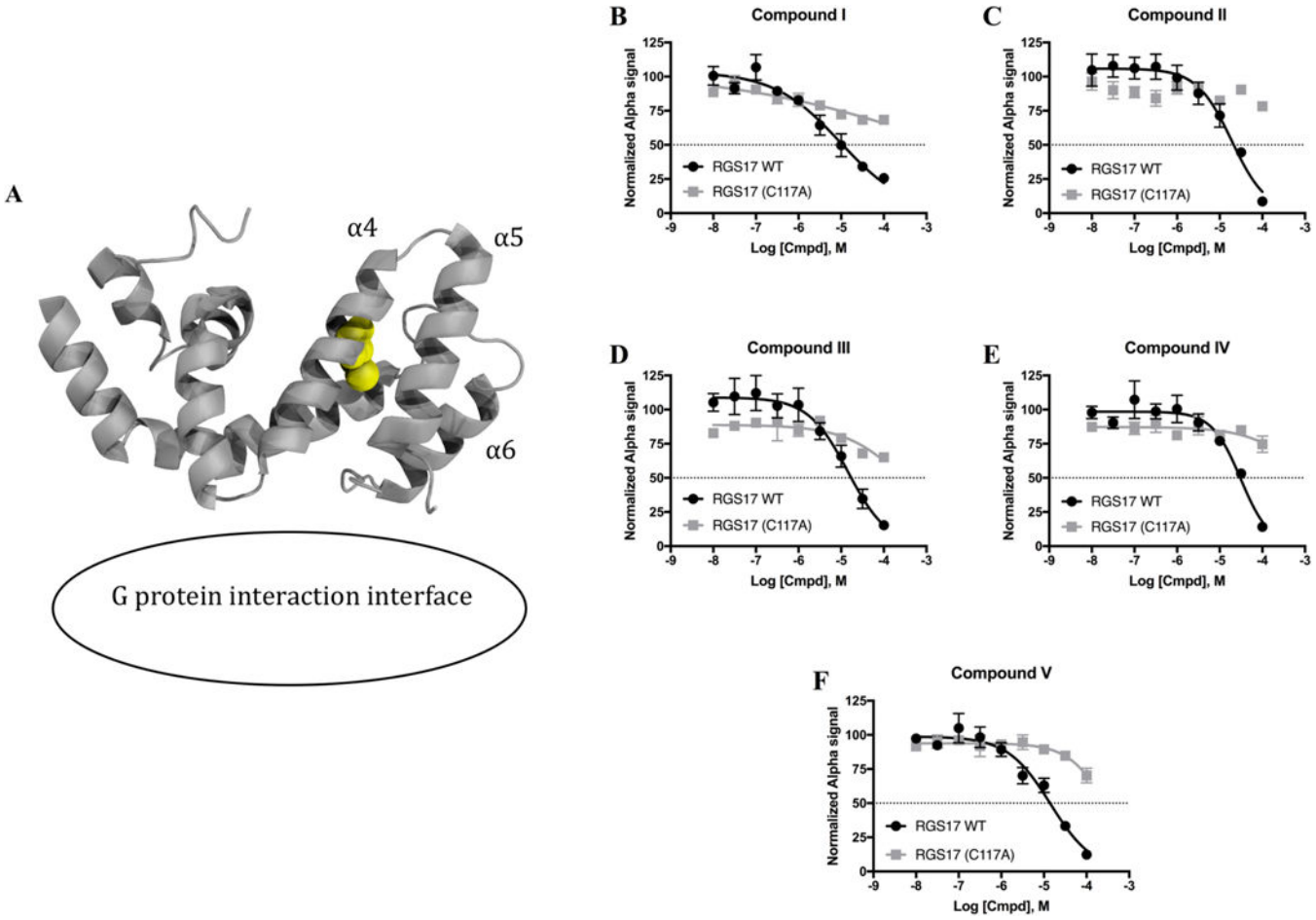

Figure 2 –.

A) Crystal structure of RGS17 (PDB - 1ZV4). G protein interaction interface is noted, and the allosteric Cys 117 is represented as spheres in yellow. B–F) Dose response analysis of the 5 lead compounds against WT and mutant protein. WT IC_{50} values were 9.5 μM, 19.2μM, 14.4 μM, 31.1 μM, and 14.3 μM for panels B–F respectively. No compound inhibited mutant RGS17 (C117A) by the highest concentration tested (100 μM). WT data are n=3 in duplicate, mutant data are n=2 in duplicate. All data shown as mean ± SEM.

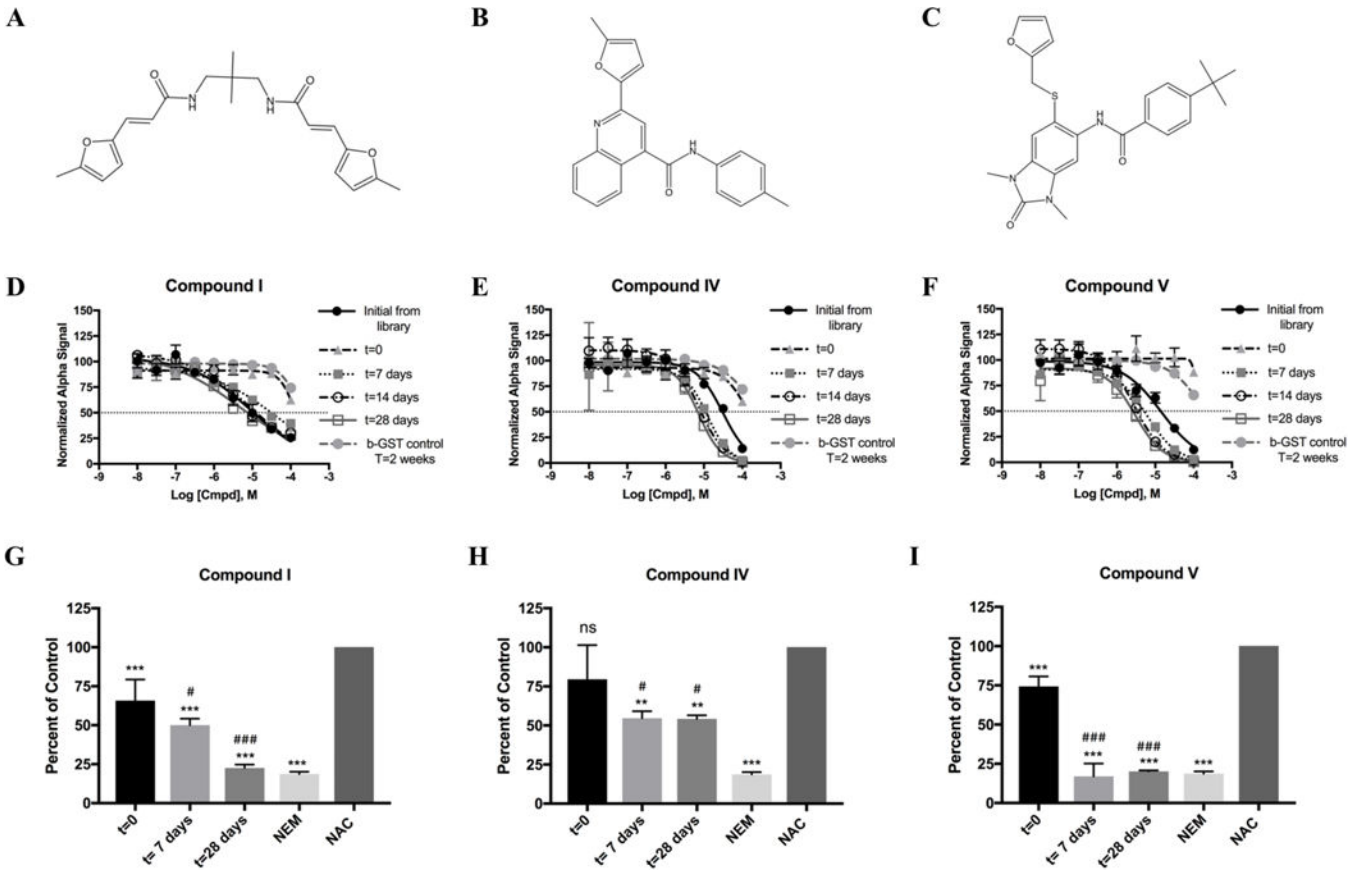

Figure 3 -

Three lead compounds decompose in DMSO. Compounds are depicted above their representative dose response analysis. Initial from library data are n=3 in duplicate. All other data are n=2 in duplicate. All dose response data shown as mean ± SEM. Panels G-I are the thiol reactivity results for the compound products over time. All data normalized to NAC alone (negative control), NEM represents positive control. Significance calculated via one way ANOVA. Holm-Sidak multiple comparison analysis shown on graph with respect to NAC control (*) and with respect to t=0 (#). P-values are */# - $P \leq 0.05$, **/## - $P \leq 0.01$, ***/### - $P < 0.001$. Thiol reactivity data are n=3.

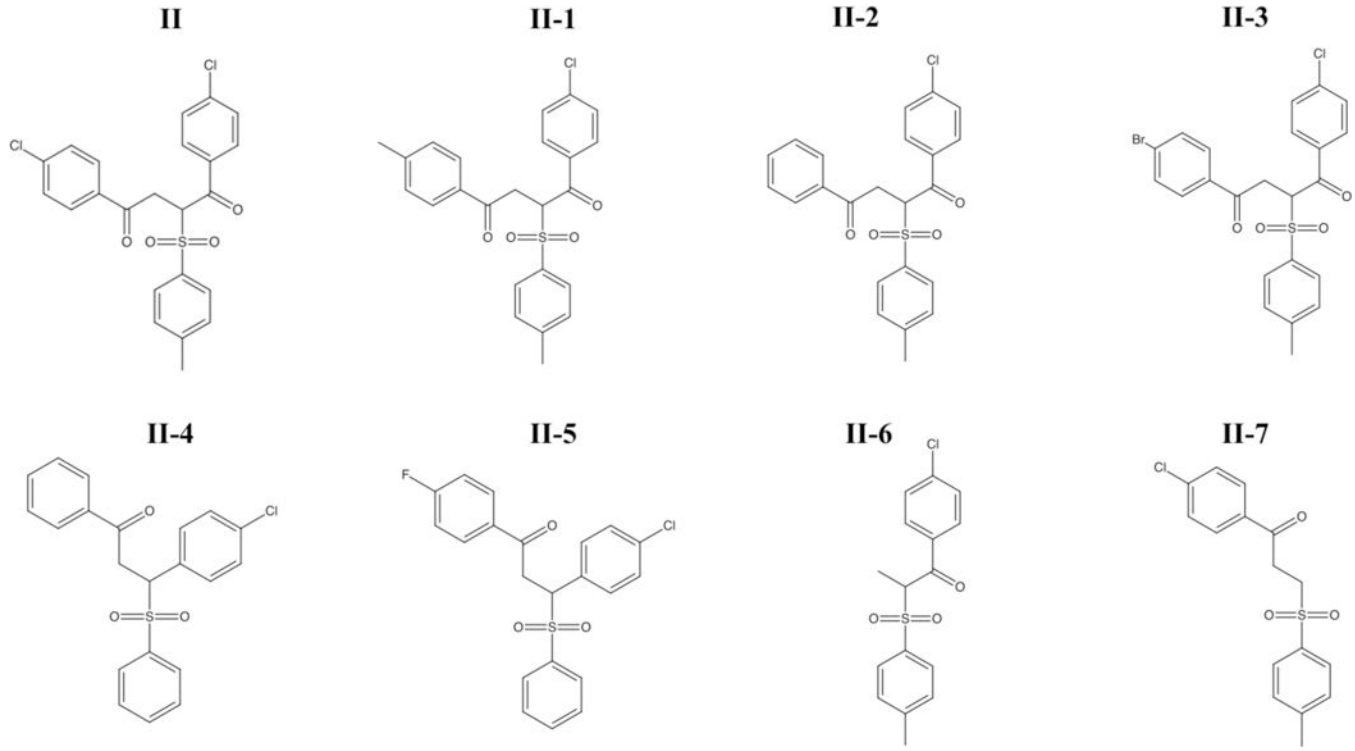

Figure 4 -
Analogs of Compound II tested in Figure 5.

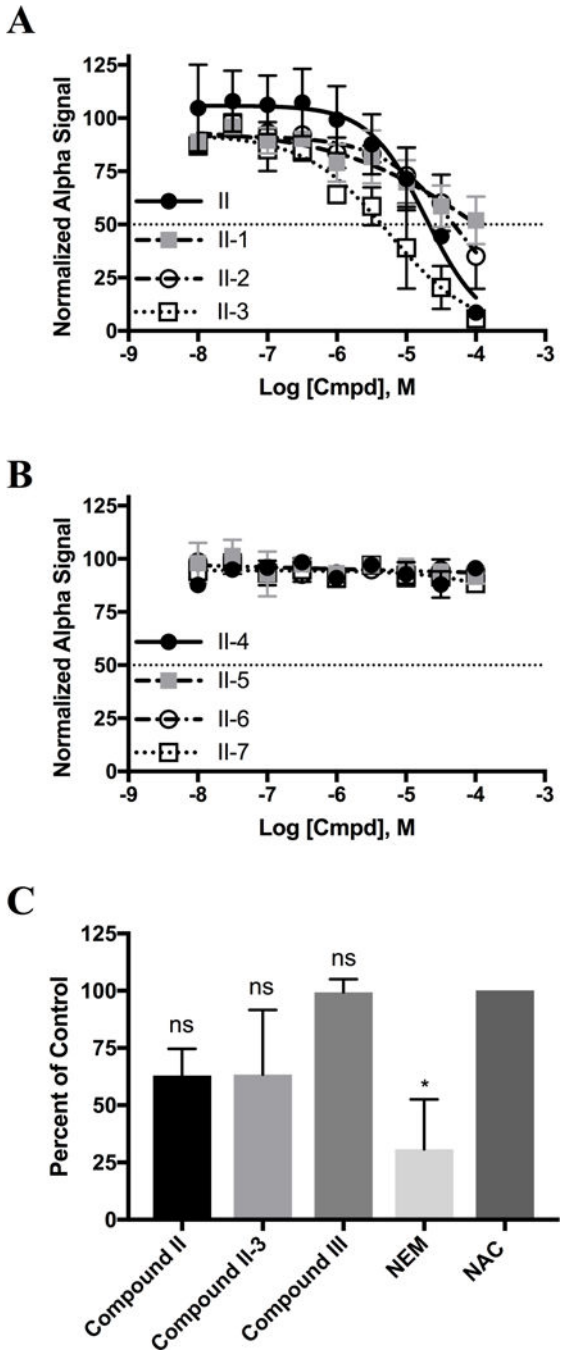

Figure 5 -

(A and B) Dose response analysis of analogs depicted in Figure 4. IC_{50} values listed in Table SV. Data are n=3 in duplicate shown as mean ± SD. (C) Thiol reactivity of Compound II, Compound II-3, and Compound III. All data normalized to NAC alone (negative control), NEM represents positive control. A statistically significant difference between the groups was determined via one way ANOVA ($F(4,13) = 6.376$, $p = 0.05$). Holm-Sidak multiple comparison analysis shown on graph with respect to NAC control (*). Thiol reactivity data are n=3.

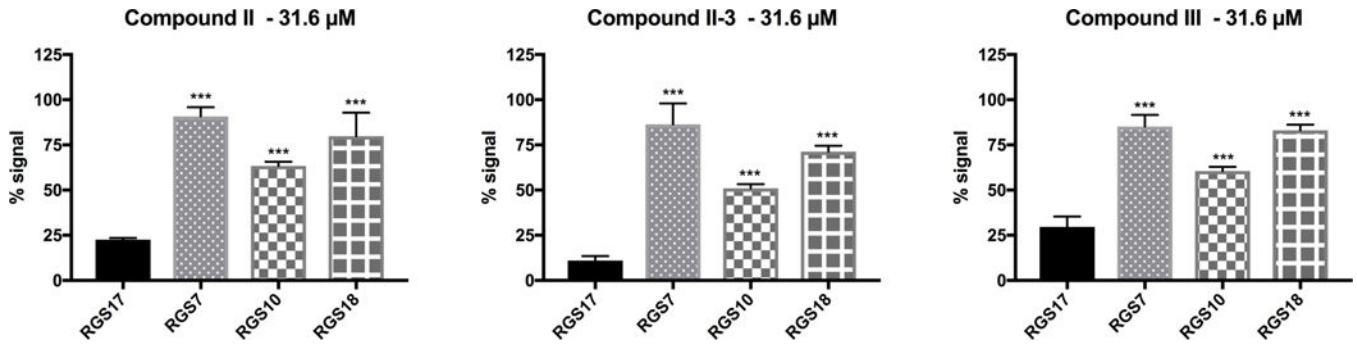

Figure 6 –.

Compound II, II-3, and III were tested for selective inhibition of RGS17 over RGS7, RGS10, and RGS18. For all three compounds, RGS17 was the most potently inhibited, with a statistically significant reduction in signal compared to the inhibition observed for RGS7, RGS10, and RGS18. Significance determined via one way ANOVA with Holm-Sidak multiple comparison post hoc analysis. Significance shown on graph are the multiple comparison analysis with respect to RGS17, *** - $P < 0.001$. Data are $n=3$ in duplicate ± SD.